Effect of Chronic Hyperglycemia on Glucose Metabolism in Subjects with Normal Glucose Tolerance

Chris Shannon PhD[1*], Aurora Merovci MD[1*], Juan Xiong[1], Devjit Tripathy MD[1], Felipe Lorenzo MD PhD[2], Donald McClain MD PhD[2], Muhammad Abdul-Ghani MD PhD[1], Luke Norton PhD[1], Ralph A DeFronzo MD[1].

[1]Division of Diabetes, University of Texas Health Science Center and Texas Diabetes Institute, San Antonio, Texas

[2] Centre of Diabetes, Obesity and Metabolism, Wake Forrest University, Winston-Salem, North Carolina

*These authors contributed equally

Key words: Insulin resistance, glucose oxidation, non-oxidative glucose disposal, glucotoxicity.

Running Title: Hyperglycemia and glucose disposal in healthy subjects

Corresponding Author:
Ralph A DeFronzo, MD
Division of Diabetes, UTHSCSA, 7703 Floyd Curve Dr.
San Antonio, TX, 78229
Phone (210) 567 6691
Fax (210) 567 6554
albarado@uthscsa.edu

Word Count:
Manuscript (n = 4233)
Abstract (n =202)
Figures (n = 6)
Tables (n = 2)

Diabetes Publish Ahead of Print, published online September 13, 2018

ABSTRACT

Chronic hyperglycemia causes insulin resistance, but the inheritability of glucotoxicity and the underlying mechanisms are unclear. We examined the effect of 3 days of hyperglycemia on glucose disposal, enzyme activities, insulin signaling and protein O-GlcNAcylation in skeletal muscle of individuals without (FH-) or with (FH+) family history of type 2 diabetes.

Twenty-five subjects with normal glucose tolerance received a [3-^{3}H]-glucose euglycemic insulin clamp, indirect calorimetry, and vastus-lateralis biopsies before and after 3-days of saline (n=5) or glucose (n=10 FH-; 10 FH+) infusion to raise plasma glucose by ~45 mg/dL.

At baseline, FH+ had lower insulin-stimulated oxidative (GOX) and total (TGD), but similar non-oxidative (NOGD) glucose disposal and basal endogenous glucose production (EGP) compared to FH-. Following three days of glucose infusion, basal EGP and GOX were markedly increased, whilst NOGD and TGD were lower versus baseline, with no differences between FH- and FH+ subjects. Hyperglycemia doubled skeletal muscle glycogen content and impaired activation of glycogen synthase, pyruvate dehydrogenase and Akt, but protein O-GlcNAcylation was unchanged.

Insulin resistance develops to a similar extent in FH- and FH+ subjects following chronic hyperglycemia, without increased protein O-GlcNAcylation. Decreased NOGD due to impaired glycogen synthase activation appears to be the primary deficit in skeletal muscle glucotoxicity.

INTRODUCTION

Insulin resistance is a core defect in type 2 diabetes (T2D) (1, 2) and is the first metabolic abnormality detected in subjects destined to develop T2D (3, 4). Insulin resistant individuals manifest diminished insulin-stimulated glucose disposal in skeletal and cardiac muscle (5-7), adipocytes (8), liver (9), and gastrointestinal tract (10). In skeletal muscle the defect in insulin action involves multiple intracellular steps in glucose metabolism including glucose oxidation and glycogen synthesis (1, 2, 11, 12). The etiology of insulin resistance is complex and includes both genetic and acquired factors (2).

Studies in experimental animals (13, 14) and in man (15, 16) have demonstrated that chronic elevation in the plasma glucose concentration impairs insulin action, i.e. glucotoxicity (17). Lowering the plasma glucose concentration with insulin therapy (18) or by inhibition of renal glucose absorption (19) improves insulin sensitivity in T2D individuals. The improvement in insulin sensitivity observed with intensive insulin therapy was due to an increase in non-oxidative glucose disposal (18), suggesting that glucotoxicity impairs insulin action by impairing glycogen synthesis. However, the molecular events underlying the development of insulin resistance and alterations in intracellular glucose metabolism in response to glucotoxicity remain poorly characterized.

Glycogen synthase (GS) and pyruvate dehydrogenase (PDH) are the rate-limiting enzymes in the regulation of non-oxidative glycogen synthesis and glucose oxidation, respectively. An additional route of skeletal muscle glucose metabolism involves synthesis of the hexosamine product O-linked β-N-acetylglucosamine (O-GlcNAc), a pathway that appears to be upregulated in T2D and has previously been implicated in the development of insulin resistance and glucotoxicity (20, 21, 22). Prior studies suggest that both glycogen synthase (23) and

pyruvate dehydrogenase (24) may be modulated by O-GlcNAcylation and thus could be sensitive to increased O-GlcNAc synthesis, but whether O-GlcNAc levels respond to chronic hyperglycemia in humans is unclear. Therefore, the aim of the present study was to examine the effect of chronic (3 days) elevation of the plasma glucose concentration on oxidative and non-oxidative glucose disposal, as well as the prospective involvement of glycogen synthase, pyruvate dehydrogenase and O-GlcNAcylation, in lean healthy, normal glucose tolerant subjects with and without family history (FH) of diabetes. We hypothesized that experimental hyperglycemia would alter the intracellular pathways of glucose metabolism in normal glucose tolerant (NGT) subjects and, based upon previous studies (25), that these changes would be more pronounced in subjects with FH of diabetes.

RESEARCH DESIGN AND METHODS

Subjects

Twenty-five NGT subjects (15 without FH of T2DM; 10 with FH) participated in the study. All subjects were in good general health as determined by medical history, physical exam, screening lab tests, urinalysis, and EKG. Body weight was stable (±3 pounds) in all subjects for 3 months prior to study and no subject was considered excessively active or sedentary. No subject was taking any medication known to affect glucose metabolism. Family history positive was defined as ≥2 first degree relatives (mother, father, siblings, children) with T2DM, ascertained by recall during the screening visit. Family history negative subjects (including saline controls) had no first degree relatives with T2DM.

Research Design

All studies were performed on the Clinical Research Center at the South Texas Veterans Health Care System at 7AM following a 10-hour overnight fast and after abstention from strenuous exercise or alcohol consumption for 48 hours. After screening, eligible subjects received a 4-hour euglycemic insulin clamp (26) with indirect calorimetry, vastus lateralis muscle biopsies, and 3-^{3}H-glucose infusion. Skeletal muscle biopsies were obtained from the vastus lateralis muscle approximately one hour prior to and at the end of the insulin clamp and were snap-frozen in liquid nitrogen. Within 7 days subjects returned to the CRC for a three day continuous glucose (n=20) or saline (n=5) infusion study. At 7 AM on day four, the glucose infusion was discontinued and the euglycemic insulin clamp with indirect calorimetry, 3-^{3}H-glucose, and vastus lateralis muscle biopsy was repeated.

Euglycemic Insulin Clamp

A catheter was placed into an antecubital vein for the infusion of all test substances. A second catheter was inserted retrogradely into a vein on the dorsum of the hand, and the hand was placed into a thermoregulated box heated to 70°C. All subjects received a prime (40 μCi)-continuous (0.4 μCi/min) infusion of 3-^{3}H-glucose (DuPont NEN Life Science Products, Boston, MA). After a 2-hour basal tracer equilibration period, subjects received a prime-continuous insulin infusion at the rate of 80 mU/m^{2}·min. During the last 30 min of the basal equilibration period and throughout the insulin infusion, plasma samples were taken at 5-10 minute intervals for determination of plasma glucose and insulin concentrations and tritiated glucose radioactivity. During the insulin infusion, a variable infusion of 20% glucose was adjusted, based on the

negative feedback principle, to maintain the plasma glucose concentration at ~100 mg/dl with a coefficient of variation <5%.

Three-day Glucose Infusion

Subjects were admitted at 8 AM for the 3-day glucose (n=20) or saline (n=5) infusion study. A catheter was placed into an antecubital vein and a variable infusion of 20% glucose was started to raise and maintain the plasma glucose concentration to ~45 mg/dl above the fasting level. Plasma glucose was measured every 5-30 minutes and the glucose infusion rate was adjusted to maintain the plasma glucose concentration at the target ±5 mg/dl. Fasting plasma insulin, FFA and C-peptide were measured in the morning of days 1, 2, 3 and 4. On the morning of day 4 the glucose infusion was discontinued, at which time the prime-continuous infusion of 3-^{3}H-glucose was initiated. The plasma glucose concentration was subsequently allowed to return to the fasting level, at which time the euglycemic insulin clamp with vastus lateralis muscle biopsy, tritiated glucose, and indirect calorimetry was then repeated. In all subjects the plasma glucose concentration returned to the baseline fasting level within 2-3 hours and the glucose specific activity was constant for 30 minutes prior to insulin infusion (see Supplemental Figure S1). During the glucose infusion period, subjects received a standardized diet (55% carbohydrate, 30% fat, 15% protein) with calories divided as 20% for breakfast and 40% each for lunch and dinner. Breakfast was not permitted on the morning of Day 4. Subjects were encouraged to ambulate during the 3-day glucose infusion period.

Analytical Determinations

Plasma glucose concentration was determined by glucose oxidase method (Analox Glucose Analyzer, Analox Instruments, Lunenburg, MA). Plasma insulin concentration was determined by radioimmunoassay (Diagnostic Products, Los Angeles, CA). Plasma tritiated glucose radioactivity was determined on barium hydroxide/zinc sulfate–precipitated plasma extracts. A ~20 mg portion of muscle was analyzed for pyruvate dehydrogenase activation status (27). An aliquot of homogenate was removed and frozen for the determination of the expression level of the following proteins by western blotting: pyruvate dehydrogenase E1α (CST #3205), pE1α (Ser^{293}; Abcam #92696), PDK4 (Abcam #110336), Akt (CST #4691), pAkt (Ser^{473}; CST #9271), glycogen synthase (CST #3886), pGS (Ser^{641}; CST #3891), GSK3β (CST #9315), pGSK3β (Ser^{9}; CST #9323), GFAT1 (CST #5322) and OGT (CST #24083). Global protein O-GlcNAcylation was assessed by western blotting using the CTD110.6 antibody (CST #9875), with visible bands quantified individually and summed for each lane. A second portion of muscle (~50 mg) was freeze-dried and extracted in 0.5M perchloric acid followed by alkaline digestion for the determination of acid soluble and acid insoluble metabolites (28). Glucose-6-phosphate was assayed by the fluorometric detection of NADH in the presence of 50mM triethanolamine, 0.5mM DTT, 0.25mM ATP, 1mM NAD and 0.6U bacterial G6PDH (Sigma G5760). Glycogen (28) and long-chain acyl CoA (29) were measured as described previously.

Calculations and Statistical Analysis

The basal rate of endogenous (primarily hepatic) glucose production (bEGP) was calculated as the [3-^{3}H] glucose infusion rate (dpm/min) divided by the steady-state plasma [3-^{3}H] glucose specific activity (dpm/mg). After insulin infusion, non-steady state conditions for [3-^{3}H] glucose prevail and total rate of glucose appearance (Ra) in the systemic circulation was computed using

Steele's equation during the last 30 minutes of the 4-hour insulin clamp, assuming a constant distribution volume of 250 mg/kg BW (30). The residual rate of endogenous glucose production (rEGP) during the last 30 minutes of the clamp step was calculated by subtracting the glucose infusion rate from Ra during the same time period. Indirect calorimetry was performed during the 30 minutes before the start of the clamp (-30-0 minutes) and during the last 30 minutes of the insulin infusion (210-240 minutes). Glucose and lipid oxidation were calculated using the non-protein respiratory exchange ratio (RER) (31). Non-oxidative glucose disposal was calculated by subtracting the rate of glucose oxidation from total glucose disposal during the insulin clamp. Units for glucose production, glucose oxidation and non-oxidative glucose disposal are normalized to body weight, given as milligrams of glucose per kilogram body weight per minute (mg/kg·min). Values are presented as the mean ± SEM. Differences between means were tested with repeated and mixed-model ANOVA, as described in figure legends. Statistical significance was determined at $P < 0.05$.

RESULTS

Subjects Characteristics and OGTT

Table 1 presents baseline patient characteristics. Subjects were well matched for age, BMI, and gender. Subjects with positive family history (FH+) had a slightly, although not significantly, higher fasting plasma glucose concentration and rise in plasma glucose concentration during the OGTT (Figure 1). Consistent with previous studies, FH+ subjects had significantly greater increase in plasma insulin concentration during the OGTT (Figure 1). Body weight and BMI were similar in FH-, FH+, and control groups.

Baseline Euglycemic Insulin Clamp

During the baseline insulin clamp, the steady state plasma insulin (163±2 vs 172±12 μU/ml) and glucose (94.8±1.8 vs 95.9±1.6) concentrations were similar in FH negative and FH positive groups, respectively. During the baseline insulin clamp, the basal rate of EGP was comparable in FH- and FH+ subjects and residual EGP during the insulin clamp was similarly suppressed in both groups (Table 2).

Consistent with previous studies (3), FH+ subjects had a significantly lower rate of total body insulin-stimulated glucose disposal during the baseline insulin clamp compared to FH- subjects (Table 2). The basal rate of glucose oxidation was comparable in FH+ and FH- groups, but during the insulin clamp glucose oxidation increased more ($P<0.05$) in FH- subjects (by 105%) than in FH+ subjects (by 64%) (Table 2).

Post 3-Day Glucose Infusion

FPG concentration on day 1 before the start of glucose infusion was 95±3 and 102±2 mg/dl in FH- and FH+ subjects, respectively ($P=0.05$) and increased similarly on days 2, 3 and 4 in FH+ and FH- subjects (144±6 vs 148±7, 139±4 vs 148±3 and 139±4 vs 135±98 mg/dl, respectively, all $p<0.001$ vs baseline) (Figure 2). After stopping the glucose infusion on day 4, the plasma glucose concentration decreased to 100±2 and 99±3 mg/dl in FH- and FH+ subjects, respectively, prior to the start of the repeat insulin clamp study. Fasting plasma insulin concentration before the start of glucose infusion was 8±3 and 12±2 μU/ml in FH- and FH+, respectively ($p>0.3$) and progressively increased to 26±6 vs 44±7, 49±15 vs 61±9, and 52±15 vs 65±11 on days 2, 3, and 4 in FH- and FH+ subjects, respectively (all $P<0.05$ vs baseline and P=NS for FH- vs FH+) (Figure 2). Fasting plasma FFA before the start of glucose infusion was

0.50±0.06 and 0.45±0.06 mmol/L in FH- and FH+, respectively, and suppressed similarly to 0.08±0.01 vs 0.06±0.01, 0.06±0.01 vs 0.07±0.01 and 0.07±0.01 vs 0.07±0.02 mmol/L on days 2, 3, and 4 (Figure 2).

In subjects who received saline infusion, the FPG, fasting plasma insulin and fasting plasma FFA concentrations remained unchanged throughout the study period (Figure 2).

Effect of Glucose Infusion on Insulin Sensitivity

The fasting plasma glucose concentration in the morning of day 4 (before the start of the repeat insulin clamp) was comparable in FH- and FH+ groups: 100±2 and 99±3 mg/dl, respectively. The basal rate of EGP increased markedly after 3 days of glucose infusion ($p<0.001$ vs baseline) and was comparable in FH- and FH+ groups (Table 2). The basal rate of glucose oxidation was significantly increased in both groups following glucose infusion, while the basal rate of lipid oxidation was decreased markedly ($P<0.001$) in both groups (Table 2).

During the insulin clamp performed after 3 days of glucose infusion, the steady state plasma glucose (96±2, 98±1, 97±2 mg/dl) concentrations were similar to those in the baseline study in FH-, FH+, and control groups, respectively, while the steady state plasma insulin concentration increased similarly and significantly in FH- (208±24) and FH+ (198±10) versus control (121±8 uU/ml) groups.

After 3 days of glucose infusion, total body insulin-mediated glucose disposal was significantly decreased in FH- subjects (from 11.49±0.9 to 9.46 ±0.69 mg/kg.min, P=0.02) while a modest, non-significant decrease was observed in FH+ subjects (from 9.32±.0.49 to 8.12± 0.55, P=0.08) (Table 2 and Figure 3). Despite the decrease in total body glucose disposal (TGD) in FH- subjects, glucose oxidation during insulin infusion was markedly increased (from 2.75±0.53

to 5.12±0.37 mg/kg•min, p<0.0001), while non-oxidative glucose disposal was markedly diminished (8.69±0.72 to 4.28±0.60 mg/kg•min, p<0.001). Although TGD was not significantly reduced by glucose infusion in FH+ subjects, oxidative (increased) and non-oxidative (decreased) glucose disposal were affected similarly to those in FH- subjects: oxidative glucose disposal increased by 142% (p<0.001) and non-oxidative glucose disposal decreased by 45% (p<0.001) in FH+ subjects (Table 2 and Figure 3).

In control subjects basal EPG, suppression of EGP during the insulin clamp, and insulin-stimulated TGD, glucose oxidation, and non-oxidative glucose disposal did not differ after 3 days of saline infusion (Table 2).

Skeletal Muscle Responses to Glucose Infusion

Consistent with the finding that both oxidative and non-oxidative pathways of glucose metabolism were similarly altered in FH- and FH+ subjects following glucose infusion, skeletal muscle biopsy molecular analyses revealed no differences between FH- and FH+ groups following experimental hyperglycemia (Supplemental Figure S2). As such, the main effects of glucose infusion are presented collectively for FH- and FH+ subjects for clarity.

Glycogen Synthase Regulation

Non-oxidative glucose disposal in skeletal muscle primarily represents glycogen synthesis (32). During the insulin clamp performed prior to the 3 day glucose infusion, muscle glycogen (mmol/kg dry weight) increased from 341±34 to 430±43 and 347±19 to 400±33 in FH- and FH+ subjects, respectively (both p<0.05) (Figure 4A).

Following 3 days of glucose infusion muscle glycogen was increased by approximately 100% in both FH- and FH+ groups ($p<0.0001$), but remained stable in the saline infusion control subjects (Figure 4A). Glycogen synthase (GS) phosphorylation (Ser^{641}) following glucose infusion was also increased, both under basal conditions and during the insulin clamp ($p=0.03$) (Figure 4B). Moreover, phosphorylation of GSK3β (Ser^{9}), the primary isoform of the regulatory GS kinase in skeletal muscle, tended to be reduced ($p=0.07$) (Figure 4C). Together, these observations are consistent with an overall inhibition of GS activation. Skeletal muscle levels of glucose-6-phosphate were unchanged following glucose infusion (Figure 4D).

Pyruvate Dehydrogenase Activation

The pyruvate dehydrogenase (PDH) complex represents a key regulatory enzymatic step in the intracellular fate of glucose, coupling glycolytic and oxidative pathways of carbohydrate metabolism. Consistent with the increased rate of glucose oxidation, the protein expression of pyruvate dehydrogenase kinase 4 (PDK4), the primary kinase responsible for the phosphorylation and inactivation of skeletal muscle PDH, was reduced by 61% ($P<0.001$) following glucose infusion (Figure 5A). Despite the reduction in PDK4, phosphorylation (Ser^{293}) of the E1α subunit of PDH was unchanged (Figure 5B) and, in agreement with the latter, the basal activation status of PDH was comparable to baseline (i.e., before glucose infusion; Figure 4C). However, glucose infusion resulted in a 20% reduction in insulin-stimulated PDH activation compared to baseline ($P=0.02$) (Figure 4C).

Insulin Signaling

To examine whether the perturbed activation of GS and PDH following glucose infusion could be related to upstream insulin signaling evens, we measured muscle Akt protein phosphorylation. During the baseline insulin clamp performed prior to glucose infusion, insulin increased muscle Akt phosphorylation (Ser473) by 12-fold (Figure 5D) ($P<0.001$). However, insulin-stimulated Akt phosphorylation was blunted by 27% ($p=0.03$) following glucose infusion, compared to baseline (Figure 5D).

Given the association between the accumulation of toxic lipid intermediates and the development of skeletal muscle insulin resistance (6), particularly under conditions of increased carbohydrate availability, we also measured the total content of long-chain acyl-CoAs (LCAC). However, glucose infusion had no impact upon either the basal (7.8 ± 1.3 vs 7.0 ± 1.0; $P=0.2$) or insulin-stimulated (10.4 ± 1.7 vs 7.1 ± 0.8 umol/kg/dw; $P=0.2$) concentrations of LCAC.

GFAT, OGT and Protein O-GlcNAcylation

Prior evidence has suggested a role for the hexosamine biosynthesis pathway in the development of skeletal muscle insulin resistance, particularly through the post-translational modification of proteins by O-GlcNAcylation (33). However, we found that 3 days of glucose infusion had no impact on global O-GlcNAcylated protein levels in skeletal muscle (Figure 6A and B). We also measured the protein levels of glutamine: fructose-6-phoshate amidotransferase 1 (GFAT1), the first and rate-limiting enzyme in hexosamine biosynthesis, as well as O-GlcNAc transferase (OGT), the rate-limiting enzyme in protein O-GlcNAcylation. Consistent with the lack of increase in O-GlcNAc levels, neither GFAT1 (Figure 6C), nor OGT (Figure 6D) protein expression were altered following 3 days of glucose infusion.

DISCUSSION

The results of the present study demonstrate that a small physiologic (~45 mg/dl) elevation in plasma glucose concentration for only 3 days exerts multiple and marked effects on hepatic and peripheral glucose metabolism in lean healthy NGT individuals with and without family history of type 2 diabetes. Although the reduction in insulin-stimulated TGD did not reach statistical significance in the FH- group (13% decrease, P=0.08), the directional change was similar to that in the FH+ group (18% decrease, P<0.001) and both insulin-stimulated glucose oxidation and non-oxidative glucose disposal were similarly and significantly affected by hyperglycemia in both groups. Thus, hyperglycemia caused a marked increase in insulin-stimulated glucose oxidation in both groups (86% and 142% in FH- and FH+ subjects, respectively) and a marked decrease in non-oxidative glucose disposal which primarily represents glycogen synthesis (by 50% and 45% in FH- and FH+ subjects, respectively). These results demonstrate that hyperglycemia exerts similar deleterious effects on the intracellular pathways of glucose disposal in subjects with and without family history of diabetes. The small quantitative difference in insulin-stimulated TGD between the two groups following 3 days of experimental hyperglycemia most likely is explained by the greater degree of insulin resistance in the FH+ group observed during the baseline insulin clamp, reflecting differences in inheritable (and/or environmental) factors between the two groups. Importantly, no changes in insulin-stimulated TGD, glucose oxidation, or non-oxidative glucose disposal were observed in the control group who were treated in an identical fashion as the glucose-infused groups with the exception that they received an infusion of normal saline. This distinguishes the effects of experimental hyperglycemia from the possible influence of decreased activity during the 3-day glucose infusion period.

The results of the present study are consistent with a previous study from our group which demonstrated that a small increase (+20 mg/dl) in plasma glucose concentration in NGT FH- subjects caused a significant increase (~25%) in glucose oxidation and decrease (~35%) in non-oxidative glucose disposal (16). The greater magnitude of change in both oxidative and non-oxidative glucose disposal in FH- subjects in the present study most likely is explained by the longer duration of hyperglycemia (3 days in the present study versus 2 days in the previous study) and greater increment in plasma glucose concentration (45 vs 20 mg/dl). Thus, the results of the present study are consistent with our previous study and extend them to demonstrate that: (i) there is dose response relationship between the level of hyperglycemia and its impact on both oxidative and non-oxidative glucose disposal, and (ii) hyperglycemia affects oxidative and non-oxidative glucose disposal similarly in FH+ and FH- subjects.

Chronic elevation of plasma glucose concentration had a dramatic effect on the basal rate of EGP which was elevated by 66% and 73% in FH- and FH+ groups, respectively, despite a marked increase in the fasting plasma insulin concentration (59 vs 10 uU/ml, $p<0.001$). The results indicate that hepatic insulin resistance was induced by sustained elevation of the plasma glucose concentration. This represents a novel finding and demonstrates that chronic experimental hyperglycemia also exerts a glucotoxic effect on hepatic and/or renal glucose production (34). Because the insulin infusion rate used during the insulin clamp in the present study produced a high steady state plasma insulin concentration, EGP was near completely suppressed to the same level as that observed during the baseline insulin clamp in both groups. While it should be acknowledged that hyperglycemia might also have influenced hepatic glucose extraction, given the relatively minor contribution of splanchnic glucose uptake to total insulin-

stimulated glucose disposal (5) it is unlikely that this was a major factor in the decrement in whole-body glucose uptake.

Since elevation of plasma glucose concentration was not performed in combination with a pancreatic/somatostatin clamp, the plasma insulin concentration also rose during the 3-day glucose infusion. We previously demonstrated that chronic elevation in plasma insulin concentration affects both oxidative and non-oxidative pathways of glucose disposal in lean healthy individuals (16). Thus, hyperinsulinemia during the 3-day glucose infusion also could have contributed to the observed effects on oxidative and non-oxidative disposal in the present study. Nonetheless, the combined hyperglycemic (+45 mg/dl) hyperinsulinemic conditions in the present study more closely reflect the physiologic conditions observed in poorly controlled obese type 2 diabetic individuals.

The present results also shed light on the mechanisms via which chronic exposure to hyperglycemia causes skeletal muscle insulin resistance. In type 2 diabetic individuals, the principle manifestation of skeletal muscle insulin resistance is impaired insulin-mediated non-oxidative glucose disposal, which after 3 days of sustained hyperglycemia (and hyperinsulinemia) in the current study was reduced by ~50%. Non-oxidative glucose disposal primarily represents skeletal muscle glycogen synthesis (32), a process controlled by the activity of glycogen synthase (GS). Increased muscle glycogen concentration has been shown to increase GS phosphorylation and directly inhibit GS activity (35, 36, 37), whilst the regulation of GS activity by GSK3β occurs independently from muscle glycogen content (37). Thus, both allosteric (increased glycogen) and post-translational (phosphorylation, possibly by GSK3β) regulation of GS likely contributed to the inhibition of non-oxidative glucose disposal following 3 days of hyperglycemia. Impaired GS activity *per se* might normally be associated with an

increase in intracellular glucose-6-phosphate (G6P) concentrations and subsequent alleviation of GS inhibition by allosterism. In the current study, G6P accumulation was likely prevented by a shunting of G6P towards glycolysis and glucose oxidation (36).

Maintenance of the intracellular G6P pool following hyperglycemia suggests that sarcolemmal glucose transport may not have been a primary defect responsible for the reduction in insulin-stimulated glucose disposal. This is in contrast to what is believed to represent the rate-limiting impairment in skeletal muscle of T2D patients and offspring (38, 39). However, it is possible that changes in G6P were masked by measurement errors introduced during the tissue biopsy procedure. Moreover, insulin-stimulated Akt phosphorylation (activation) was reduced by 27% following hyperglycemia. Given that GLUT4 translocation is a primary downstream target of Akt, we cannot conclusively rule out impairment of sarcolemmal glucose transport in the development of glucotoxicity and insulin resistance with this model. Interestingly, another notable substrate for Akt in skeletal muscle is GSK3β, providing an additional mechanism through which lower Akt activity could contribute to the reduction in non-oxidative glucose disposal following hyperglycemia.

Few data exist on the regulatory role of the pyruvate dehydrogenase complex in response to sustained hyperglycemia in humans. In the current study, the changes in circulating concentrations of insulin (increased) and free fatty acids (decreased) that accompanied hyperglycemia likely contributed to the downregulation of PDK4 protein expression (40). This would be expected to favor transformation of PDH to its active form to facilitate the increase in glucose oxidation. However, neither the phosphorylation nor basal activation status of PDH were altered by glucose infusion. This discrepancy likely reflects the complex allosteric regulation of flux through the active fraction of PDH. Indeed, the marked increase in muscle glycogen

concentration and inhibition of glycogen synthase activity following glucose infusion would be expected to favor an increased rate of pyruvate formation and consequently augment PDH flux independently of activation status (41). Consistent with previous findings in rats (36), these results demonstrate how a defect in non-oxidative glucose disposal through perturbations in glycogen synthase activity can promote the subsequent shunting of glucose through glycolysis towards oxidation. Although markedly increased, the enhanced rate of glucose oxidation was still insufficient to offset the decrement in muscle glycogen synthesis and consequently insulin-stimulated whole-body glucose disposal was reduced. Interestingly, the ability of insulin to activate PDH was lost following glucose infusion which, which was consistent with the failure of insulin to stimulate any further increase in glucose oxidation and is further indicative of distal impairments in skeletal muscle insulin action.

Another pathway that may be sensitive to the shunting of glucose from non-oxidative disposal towards glycolysis is the hexosamine synthesis pathway, which has been linked with the development of glucotoxicity and insulin resistance (20, 21, 22). However, we found no evidence for an increase in glucose metabolism to hexosamines, as reflected by stable levels of protein O-GlcNAcylation, GFAT1 and OGT in skeletal muscle. It is possible that a longer duration of hyperglycemia is needed to observe upregulation of these pathways, which have previously been shown to be increased in T2D individuals (21). Another alternative route of glucose metabolism is through the lipid synthesis pathway, offering a mechanistic link between glucotoxicity and lipotoxicity. Indeed, RER values >1.0 were observed in many volunteers following glucose infusion, indicative of whole-body net lipid synthesis. However, given the sustained suppression of circulating FFA during the glucose infusion and, consistent with the lack of effect on long chain acyl-CoA concentrations, the contribution of lipogenesis

(presumably hepatic) and change in plasma lipid levels to the development of skeletal muscle insulin resistance is likely to be inconsequential.

In summary, the present study demonstrates that sustained physiologic hyperglycemia for 3 days produces marked insulin resistance in the non-oxidative (glycogen synthesis) pathway of glucose disposal while augmenting the glucose oxidative pathway. At the molecular level, perturbations in both glycogen synthase and pyruvate dehydrogenase activation play an important role in the glucotoxic effect of hyperglycemia to produce insulin resistance.

ACKNOWLEDGMENTS

The work was supported by NIH grant DK24092-34 (RAD). Dr. DeFronzo's salary is supported, in part, by the South Texas Veterans Health Care System.

AUTHORS' CONTRIBUTION

All authors contributed to performance of the study. Drs. Abdul-Ghani and DeFronzo wrote the first draft of the manuscript that subsequently was reviewed and revised by all other authors. Dr. Chris Shannon performed all of the molecular analyses and integrated the results with the *in vivo* metabolic results. Dr. Donald McClain performed the hexosamine pathway analyses.

REFERENCES

1. DeFronzo RA. Banting Lecture: From the triumvirate to the ominous octet: a new paradigm for the treatment of type 2 diabetes mellitus. Diabetes 58:773-95, 2009.

2. DeFronzo R, Ferrannini E, Groop L, Henry RR, Herman WH, Holst JJ, Hu FB, Kahn CR, Raz, I, Shulman GI, Simonson D, Testa MA, Weiss R. Type 2 diabetes mellitus. Nat Rev Dis Primer 1:15019, 2015.

3. Gulli G, Ferrannini E, Stern M, Haffner S, DeFronzo RA. The metabolic profile of NIDDM is fully established in glucose-tolerant offspring of two Mexican-American NIDDM parents. Diabetes 41:1575-1586, 1992.

4. Martin BC, Warram JH, Krolewski AS, Bergman RN, Soeldner JS, Kahn CR. Role of glucose and insulin resistance in development of type 2 diabetes mellitus: results of a 25-year follow-up study. Lancet 340:925-9, 1992.

5. DeFronzo RA, Gunnarsson R, Bjorkman O, Olsson M, Wahren J. Effects of insulin on peripheral and splanchnic glucose metabolism in non-insulin-dependent (type II) diabetes mellitus. J Clin Invest 76:149-155, 1985.

6. Bajaj M, Baig R, Suraamornkul S, Hardies LJ, Coletta D, Cline GW, Monroy A, Musi N, Shulman GI, DeFronzo RA. Effect of pioglitazone on intramocellular fat metabolism in patients with type 2 diabetes mellitus. J Clin Endo Metab 95:1916-1923, 2010.

7. Clarke GD, Solis-Herrera C, Molina-Wilkins M, Martinez S, Merovci A, Cersosimo E, Chilton RJ, Iozzo P, Gastaldelli A, Abdul-Ghani M, DeFronzo RA. Pioglitazone improves left ventricular diastolic function in diabetic subjects. Diabetes Care 40:1530-1536, 2017.

8. Gastaldelli A, Gaggini, M, DeFronzo R. Role of adipose tissue insulin resistance in the natural history of T2DM: results from the San Antonio Metabolism Study. Diabetes 66:815-822, 2017.

9. DeFronzo RA, Ferrannini E, Simonson DC. Fasting hyperglycemia in non-insulin dependent diabetes mellitus: contributions of excessive hepatic glucose production and impaired tissue glucose uptake. Metabolism 38:387-395, 1989.

10. Mäkinen J, Hannukainen JC, Karmi A, Immonen HM, Soinio M, Nelimarkka L, Savisto N, Helmiö M, Ovaska J, Salminen P, Iozzo P, Nuutila P. Obesity-associated intestinal insulin resistance is ameliorated after bariatric surgery. Diabetologia 58:1055-62, 2015.

11. Groop LC, Bonadonna RC, DelPrato S, Ratheiser K, Zyck K, Ferrannini E, DeFronzo RA. Glucose and free fatty acid metabolism in non-insulin-dependent diabetes mellitus. Evidence for multiple sites of insulin resistance. J Clin Invest 84:205-213, 1989

12. Felber JP, Ferrannini E, Golay A, Meyer HU, Theibaud D, Curchod B, Maeder E, Jequier E, DeFronzo RA. Role of lipid oxidation in pathogenesis of insulin resistance of obesity and type II diabetes. Diabetes 36:1341-50, 1987.

13. Rossetti L, Smith D, Shulman GI, Papachristou D, DeFronzo RA. Correction of hyperglycemia with phlorizin normalizes tissue sensitivity to insulin. J Clin Invest 79:1510-1515, 1987.

14. Kahn BB, Shulman GI, DeFronzo RA, Cushman SW, Rossetti L. Normalization of blood glucose in diabetic rats with phlorizin treatment reverses insulin-resistant glucose transport in

adipose cells without restoring glucose transporter gene expression. J Clin Invest 87:561-570, 1991.

15. Yki-Järvinen H, Helve E, Koivisto VA. Hyperglycemia decreases glucose uptake in type I diabetes. Diabetes 36:892-6, 1987.

16. Del Prato S, Leonetti F, Simonson DC, Sheehan P, Matsuda M, DeFronzo RA. Effect of sustained physiologic hyperinsulinemia and hyperglycaemia on insulin secretion and insulin sensitivity in man. Diabetologia 37:1025-1035, 1994.

17. Rossetti L, Giaccari A, DeFronzo RA. Glucose toxicity. Diabetes Care-Reviews 13:610-630, 1990.

18. Garvey WT, Olefsky JM, Griffin J, Hamman RF, Kolterman OG. The effect of insulin treatment on insulin secretion and insulin action in type II diabetes mellitus. Diabetes 34:222-34, 1985.

19. Merovci A, Solis-Herrera C, Daniele G, Eldor R, Fiorentino TV, Tripathy D, Xiong J, Perez Z, Norton L, Abdul-Ghani MA, DeFronzo RA. Dapagliflozin improves muscle insulin sensitivity but enhances endogenous glucose production. J Clin Invest 124:509-14, 2014.

20. Yki-Jarvinen H, Vogt C, Iozzo P, Pipek R, Daniels MC, Virkamaki A, Makimattila S, Mandarino L, DeFronzo RA, McClain D, Gottshalk K. UDP-N-Acetyl glucosamine transferase and glutatamine:fructose-6-phosphate amido transferase activities in insulin sensitive tissues. Diabetologia 40:76-81, 1997.

21. Yki-Jarvinen H, Daniels MC, Virkamäki A, Mäkimattila S, DeFronzo RA, McClain D. Increased glutamine: fructose-6-phosphate amidotransferase activity in skeletal muscle of patients with NIDDM. Diabetes 45:302-307, 1996.

22. Yki-Järvinen H, Virkamäki A, Daniels MC, McClain D, Gottschalk WK. Insulin and glucosamine infusions increase O-linked N-acetyl-glucosamine in skeletal muscle proteins in vivo. Metabolism 47:449-455, 1998.

23. Parker G, Taylor R, Jones D, McClain D. Hyperglycemia and inhibition of glycogen synthase in streptozotocin-treated mice: role of O-linked N-acetylglucosamine. J Biol Chem 279: 20636-20642, 2004.

24. Burnham-Marusich A, Berninsone P. Multiple proteins with essential mitochondrial functions have glycosylated isoforms. Mitochondrion 12: 423-427, 2012.

25. Kashyap S, Belfort R, Gastaldelli A, Pratipanawatr T, Berria R, Pratipanawatr W, Bajaj M, Mandarino L, DeFronzo RA, Cusi K. A sustained increase in plasma free fatty acids impairs insulin secretion in non-diabetic subjects genetically predisposed to develop type 2 diabetes. Diabetes 52:2461-2474, 2003.

26. DeFronzo RA, Tobin JD, Andres R. Glucose clamp technique. A method for quantifying insulin secretion and resistance. Am J Physiol 237:E214-E223, 1979.

27. Constantin-Teodosiu D, Cederblad G, Hultman E. A sensitive radioisotopic assay of pyruvate dehydrogenase complex in human muscle tissue. Anal Biochem. 198(2):347-51. 1991.

28. Harris RC, Hultman E, Nordesjö L-O. Glycogen, glycolytic intermediates and high-energy phosphates determined in biopsy samples of musculus quadriceps femoris of man at rest. Scand J Clin Lab Invest 33:109-20, 1974.

29. Cederblad G, Carlin JI, Constantin-Teodosiu D, Harper P, Hultman E. Radioisotopic assays of CoASH and carnitine and their acetylated forms in human skeletal muscle. Anal Biochem: 185:274-8. 1990.

30. Ferrannini E, Smith JD, Cobelli C, Toffolo G, Pilo A, DeFronzo RA. Effect of insulin on the distribution and disposition of glucose in man. J Clin Invest 76: 357-364, 1985.

31. Simonsen DC, DeFronzo RA. Indirect calorimetry: Methodological and interpretive problems. Am J Physiol 258: E399-412, 1990.

32. Shulman GI, Rothman DL, Jue T, Stein P, DeFronzo RA, Shulman RG. Quantitation of muscle glycogen synthesis in normal subjects and subjects with non-insulin dependent diabetes by 13C nuclear magnetic resonance spectroscopy. New Engl J Med 322: 223-228, 1990.

33. McClain DA, Crook ED. Hexosamines and insulin resistance. Diabetes 45:1003-9, 1996.

34. DeFronzo RA, Norton L, Abdul-Ghani M. Renal, metabolic and cardiovascular considerations of SGLT2 inhibition. Nat Rev Nephrol 13:11-26, 2017.

35. Danforth WH. Glycogen synthetase activity in skeletal muscle. Interconversion of two forms and control of glycogen synthesis. J Biol Chem: 240, 588-593, 1965.

36. Jensen J, Jebens E, Brennesvik EO, Ruzzin J, Soos MA, Engebretsen EM, O'Rahilly S, Whitehead JP. Muscle glycogen inharmoniously regulates glycogen synthase activity, glucose uptake, and proximal insulin signaling. Am J Physiol Endo Met: 290:E154-62, 2006.

37. Lai Y-C, Stuenæs JT, Kuo CH, Jensen J. Glycogen content and contraction regulate glycogen synthase phosphorylation and affinity for UDP-glucose in rat skeletal muscles. Am J Physiol Endocrinol Metab 293: E1622–E1629, 2007.

38. Rothman DL, Magnusson I, Cline G, Gerard D, Kahn RC, Shulman RG, Shulman GI. Decreased muscle glucose transport/phosphorylation is an early defect in the pathogenesis of non-insulin-dependent diabetes mellitus. Proc. Natl. Acad. Sci 92: 983-987, 1995.

39. Rothman DL, Schulman RG, Schulman GI. 31P nuclear magnetic resonance measurements of glucose-6-phosphate. Evidence for reduced insulin-dependent muscle glucose transport or phosphorylation activity in non-insulin-dependent diabetes mellitus. J Clin Invest 89: 1069-1075, 1992

40. Chokkalingam K, Jewell K, Norton L, Littlewood J, van Loon LJ, Mansell P, Macdonald IA, Tsintzas K. High-fat/low-carbohydrate diet reduces insulin-stimulated carbohydrate oxidation but stimulates nonoxidative glucose disposal in humans: An important role for skeletal muscle pyruvate dehydrogenase kinase 4. J Clin Endo Met: 92 284-92, 2007.

41. Constantin-Teodosiu D, Peirce NS, Fox J, Greenhaff PL. Muscle pyruvate availability can limit the flux, but not activation, of the pyruvate dehydrogenase complex during submaximal exercise in humans. J Physiol 561:647-655, 2004.

Table 1: Baseline patient characteristics. There were no significant differences between the FH-, FH+ and control groups.

	Negative FH	Positive FH	Control
Number	10	10	5
Age (years)	45±4	43±5	49±4
Gender (M/F)	7/3	6/4	2/3
Ethnicity (MA/C/AA)	3/4/3	6/3/1	1/4
BMI (kg/m^2)	24.3±1.1	26.1±1.2	24.5±1.3
Body weight (kg)	75.6±16.3	73.7±10.9	72.6±11.5
Fat-free mass (kg)	57.4±12.8	51.5±9.6	52.0±11.2
HbA1c (%)	5.4±0.1	5.4±0.1	5.4±0.1
FPG (mg/dl)	96.2±2.6	100.7±2.0	94.1±5.2
2-hour PG (mg/dl)- OGTT	95±5	109±6	111±5

Table 2: Total body glucose disposal (TGD), nonoxidative glucose disposal (NOX-GD), glucose oxidation (GOX), and endogenous (primarily reflects hepatic) glucose production (rEGP) during the insulin clamp before and after glucose infusion.

Baseline Insulin Clamp	Negative FH	Positive FH	Control
SSPG (mg/dL)	94.8±1.8	95.9±1.6	94.9±3.3
SSPI (μU/ml)	163±2	172±12	125±8
bEGP (mg/kg/min)	2.33±0.08	2.09±0.09	2.46±0.11
bEGP x basal insulin ([μU/ml]·[mg/kg/min])	20.5±1.9	19.3±4.2	19.2±1.7
TGD (mg/kg/min)	11.49±0.91	9.32±0.49*	11.18±1.64
rEGP (mg/kg/min)	0.56±0.2	0.56±0.33	0.34±0.26
Basal GOX (mg/kg/min)	1.33±0.13	1.14±0.18	1.34±0.13
Clamp GOX (mg/kg/min)	2.75±0.53	1.81±0.26*	2.45±0.17
NOX-GD (mg/kg/min)	8.69±0.82	7.46±0.61	8.35±1.88
Basal LOX (mg/kg/min)	0.92±0.10	0.94±0.09	0.99±0.19
Clamp LOX (mg/kg/min)	0.50±0.08	0.74±0.11	0.45±0.2
Basal RER	0.81±0.02	0.80±0.02	0.81±0.02
Clamp RER	0.90±0.02	0.85±0.02	0.91±0.03
Insulin Clamp Post Glucose Infusion			
SSPG (mg/dL)	96.1±2.0	98.1±1.4	96.9±2.0
SSPI (μU/ml)	208±24	198±10	121±8
bEGP (mg/kg/min)	3.87±0.37††	3.63±0.27††	2.27±0.11
bEGP x basal insulin ([μU/ml]·[mg/kg/min])	74.9±12.8††	59.1±5.5†††	20.4±1.0
TGD (mg/kg/min)	9.46±0.69†††	8.12±0.55††	10.65±1.61
rEGP (mg/kg/min)	0.54±0.22	0.47±0.11	0.14±0.09
Basal GOX (mg/kg/min)	4.64±0.39	3.78±0.25	1.35±0.18
Clamp GOX (mg/kg/min)	5.12±0.37†	4.39±0.29†	3.03±0.21
NOX-GD (mg/kg/min)	4.28±0.60†	4.11±0.69†	7.61±1.69
Basal LOX (mg/kg/min)	-0.14±0.12	0.14±0.06	0.86±0.04
Clamp LOX (mg/kg/min)	-0.15±0.12	0.09±0.08	0.42±0.11
Basal RER	1.0±0.02	0.97±0.01	0.81±0.01
Clamp RER	1.0±0.02	0.98±0.01	0.92±0.01

* $p<0.05$ FH+ versus FH-

††† $p = 0.02$ Post glucose infusion versus baseline

†† $p = 0.08$ Post glucose infusion versus baseline

† $p < 0.001$ Post glucose infusion versus baseline

FIGURE LEGENDS

Figure 1. Plasma glucose and insulin concentrations during the OGTT performed in normal glucose tolerant individuals with (FH+) and without (FH-) family history of diabetes and in the NGT control group.

Figure 2. Fasting plasma glucose (A), insulin (B) and free fatty acid (C) concentrations at baseline and during three days of either glucose infusion in normal glucose tolerant individuals without (FH+; dark bars; n=10) and with (FH+; white bars; n =10) family history of diabetes, or saline infusion in the NGT control group (grey bars; n=5). Data represent mean ± standard error and were analyzed using two-way mixed model (group x time) ANOVA. **P<0.01, ***P<0.001 vs control group and vs baseline.

Figure 3. Insulin-stimulated total body glucose disposal (total height of bars), nonoxidative glucose disposal (shaded part of bars), and glucose oxidation (GOX) in family history positive (FH+) and family history negative (FH-) individuals during the euglycemic insulin clamp performed at baseline and after 3 days of glucose infusion. Right panel shows control subjects receiving saline infusion. *p<0.05 FH+ vs FH-, † p<0.05 post-glucose infusion vs baseline.

Figure 4. Glycogen synthesis signaling: Skeletal muscle glycogen content (A) at baseline and during three days of either glucose infusion in normal glucose tolerant individuals without (FH+; dark bars; n=10) and with (FH+; white bars; n =10) family history of diabetes, or saline infusion in the NGT control group (right panel; n=5). Representative western blot images of the total and phosphorylated protein expression (top panel) and densitometry quantitation of the phos / total ratio of glycogen synthase (B) and glycogen synthase kinase 3β (C); glucose-6-phoshate (D) and glycogen (E) concentrations in skeletal muscle of all subjects receiving glucose infusion. Data are expressed as the mean ± standard error and were analyzed using two-way repeated model (clamp x infusion) ANOVA. *P<0.05, **P<0.01, ***P<0.001 for clamp vs basal; ^P<0.05, ^^^P<0.001 post-glucose infusion vs baseline.

Figure 5. Pyruvate dehydrogenase regulation and insulin signaling: Representative western blot images and densitometry quantitation of PDK4 protein expression (A), pyruvate dehydrogenase E1α subunit phosphorylation (B) and Akt phosphorylation (D) and pyruvate dehydrogenase activation status (C) at baseline (black bars) and following three days of either glucose (white bars) or saline infusion (grey bars) infusion in normal glucose tolerant subjects. Data represent mean ± standard error and were analyzed using two-way mixed model (group x clamp; group x infusion) ANOVA. *P<0.05, **P<0.01 for clamp vs basal; ^P<0.05, ^^^P<0.001 post-glucose infusion vs baseline.

Figure 6. Basal O-GlcNAcylated protein quantification before and after 3 days of saline (black bars) or glucose (white bars) infusion (A) and representative blot for three subjects receiving glucose infusion (B). Basal and insulin stimulated OGT (C) and GFAT1 (D) quantification before (black bars) and after (white bars) 3 days of glucose infusion and representative blots (E). Data represent mean ± standard error and were analyzed using two-way mixed model (group x clamp; group x infusion) ANOVA.

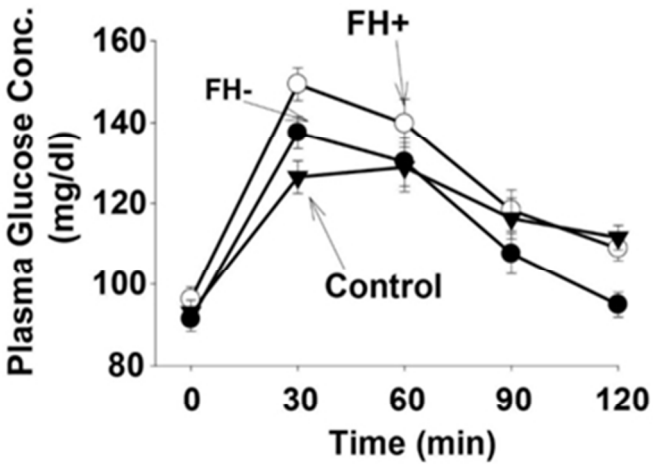

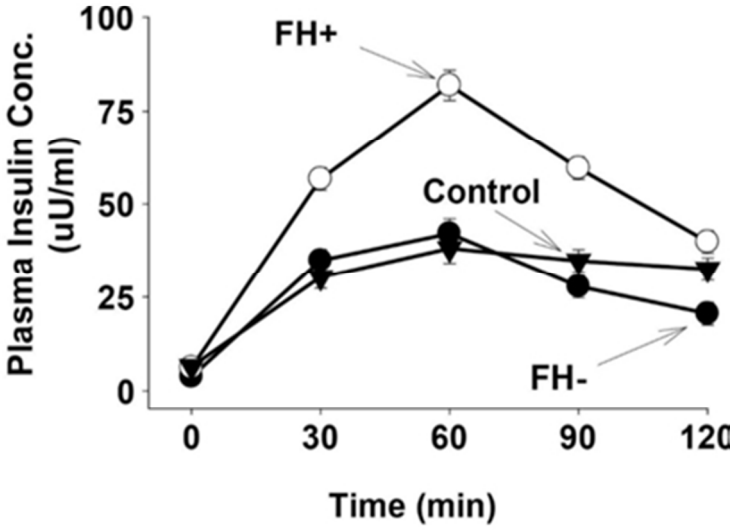

Plasma glucose and insulin concentrations during the OGTT performed in normal glucose tolerant individuals with (FH+) and without (FH-) family history of diabetes and in the NGT control group.

78x123mm (150 x 150 DPI)

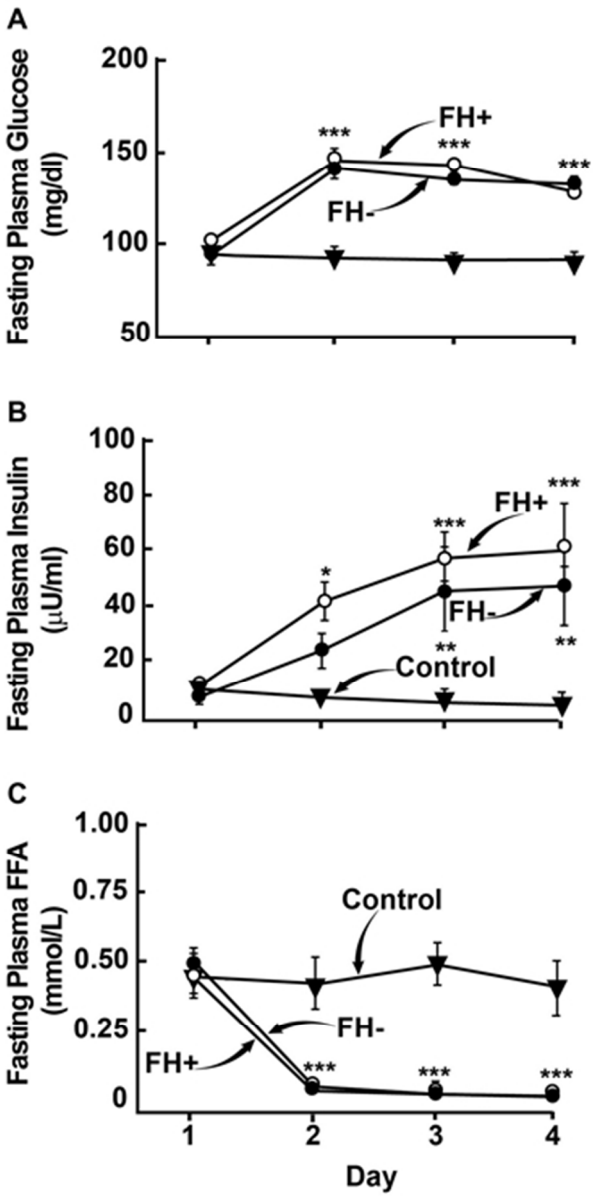

Fasting plasma glucose (A), insulin (B) and free fatty acid (C) concentrations at baseline and during three days of either glucose infusion in normal glucose tolerant individuals without (FH+; dark bars; n=10) and with (FH+; white bars; n =10) family history of diabetes, or saline infusion in the NGT control group (grey bars; n=5). Data represent mean ± standard error and were analyzed using two-way mixed model (group x time) ANOVA. **P<0.01, ***P<0.001 vs control group and vs baseline.

61x125mm (150 x 150 DPI)

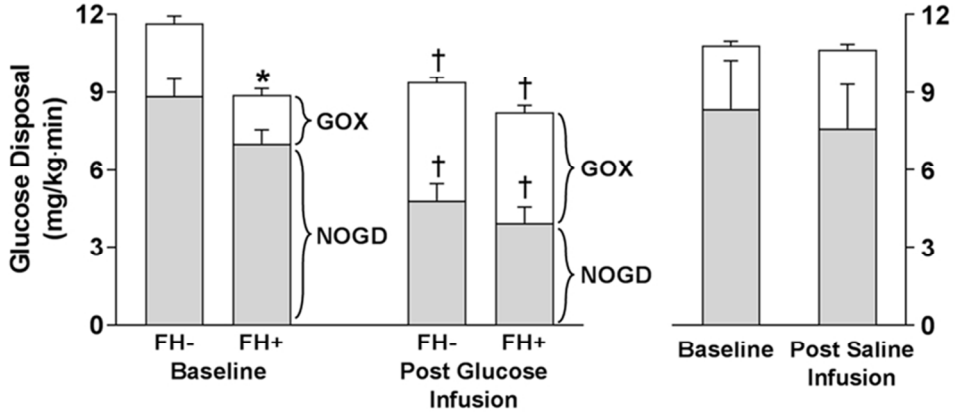

Insulin-stimulated total body glucose disposal (total height of bars), nonoxidative glucose disposal (shaded part of bars), and glucose oxidation (GOX) in family history positive (FH+) and family history negative (FH-) individuals during the euglycemic insulin clamp performed at baseline and after 3 days of glucose infusion. Right panel shows control subjects receiving saline infusion. *p<0.05 FH+ vs FH-, † p<0.05 post-glucose infusion vs baseline.

163x72mm (150 x 150 DPI)

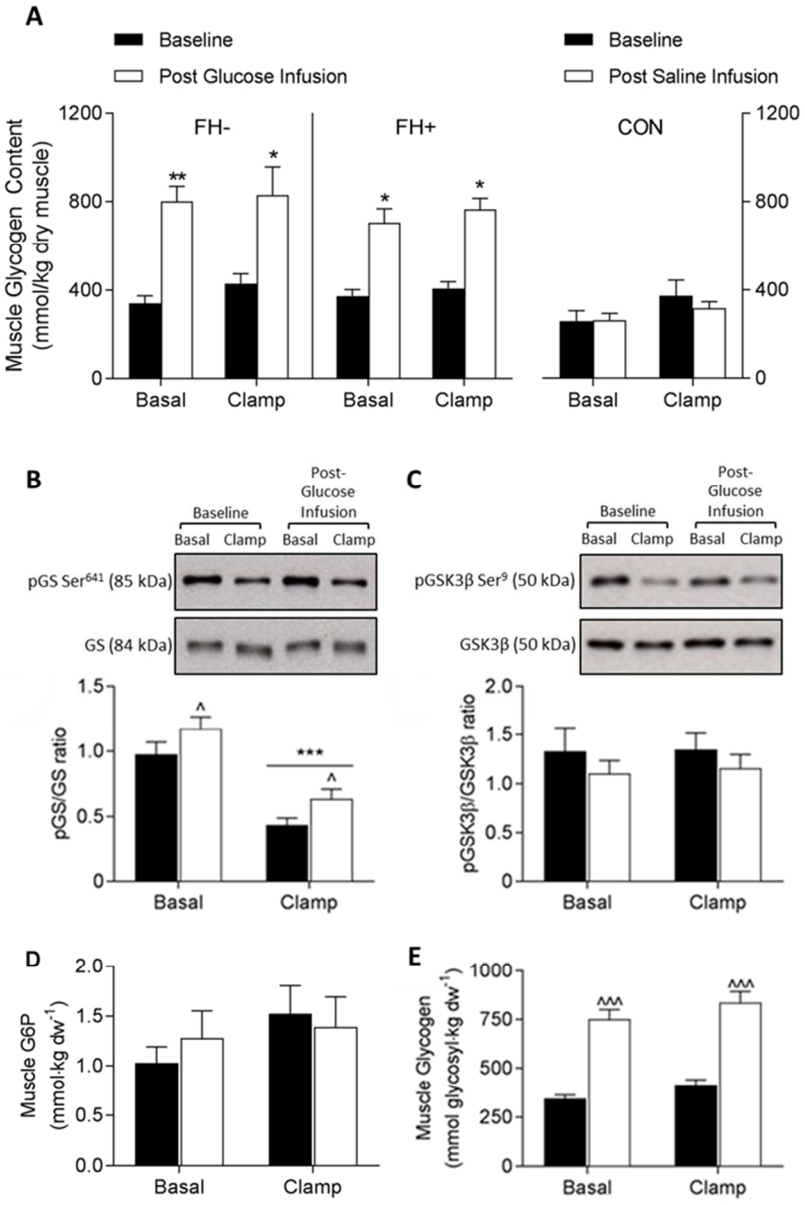

Glycogen synthesis signaling: Skeletal muscle glycogen content (A) at baseline and during three days of either glucose infusion in normal glucose tolerant individuals without (FH+; dark bars; n=10) and with (FH+; white bars; n =10) family history of diabetes, or saline infusion in the NGT control group (right panel; n=5). Representative western blot images of the total and phosphorylated protein expression (top panel) and densitometry quantitation of the phos / total ratio of glycogen synthase (B) and glycogen synthase kinase 3β (C); glucose-6-phoshate (D) and glycogen (E) concentrations in skeletal muscle of all subjects receiving glucose infusion. Data are expressed as the mean ± standard error and were analyzed using two-way repeated model (clamp x infusion) ANOVA. *P<0.05, **P<0.01, ***P<0.001 for clamp vs basal; ^P<0.05, ^^^P<0.001 post-glucose infusion vs baseline.

128x185mm (150 x 150 DPI)

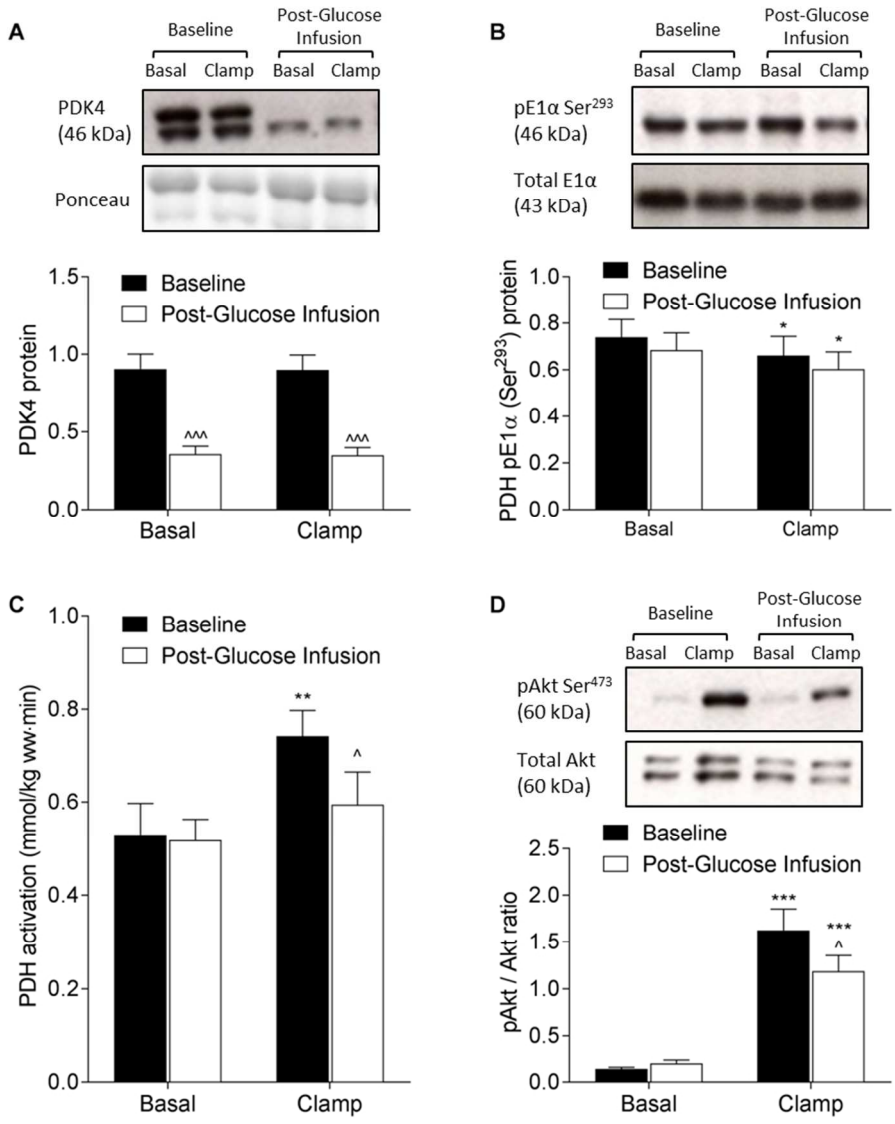

Pyruvate dehydrogenase regulation and insulin signaling: Representative western blot images and densitometry quantitation of PDK4 protein expression (A), pyruvate dehydrogenase E1α subunit phosphorylation (B) and Akt phosphorylation (D) and pyruvate dehydrogenase activation status (C) at baseline (black bars) and following three days of either glucose (white bars) or saline infusion (grey bars) infusion in normal glucose tolerant subjects. Data represent mean ± standard error and were analyzed using two-way mixed model (group x clamp; group x infusion) ANOVA. *P<0.05, **P<0.01 for clamp vs basal; ^P<0.05, ^^^P<0.001 post-glucose infusion vs baseline.

163x190mm (150 x 150 DPI)

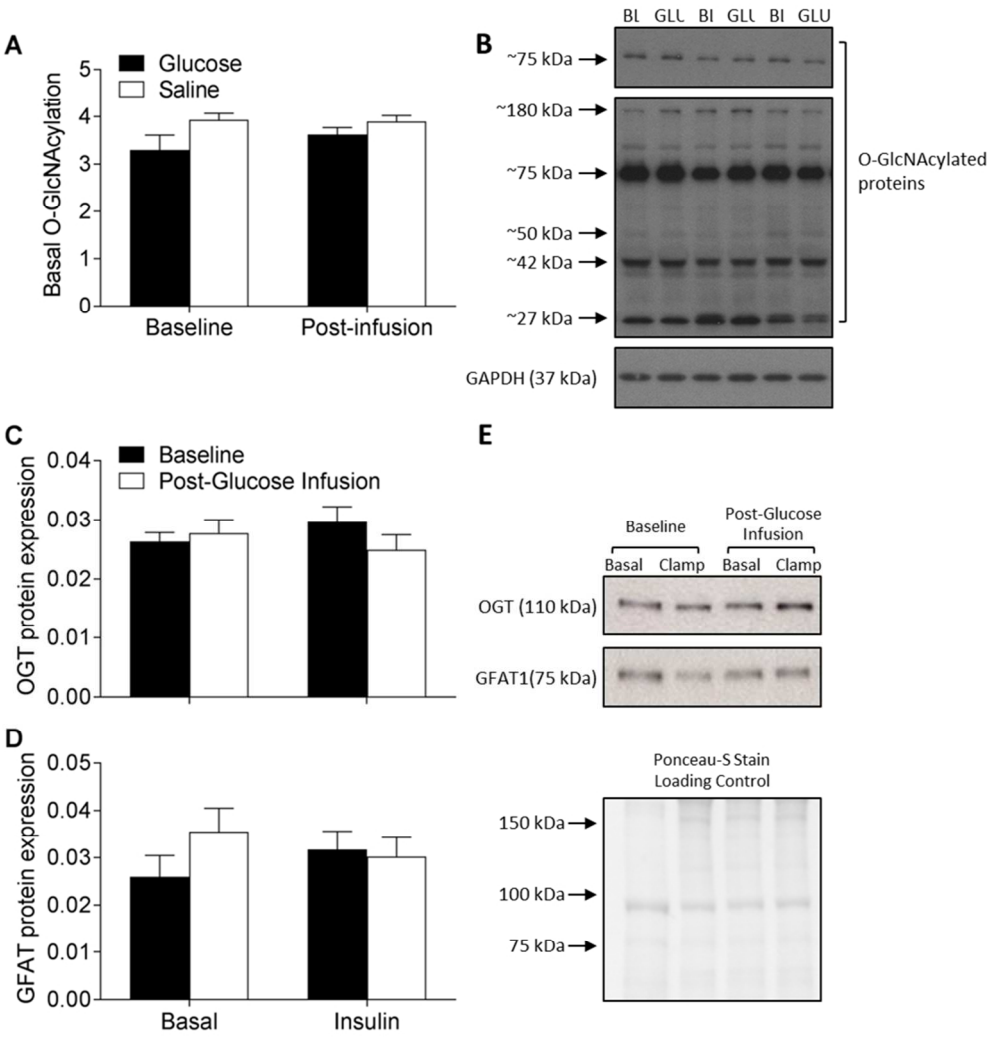

Basal O-GlcNAcylated protein quantification before and after 3 days of saline (black bars) or glucose (white bars) infusion (A) and representative blot for three subjects receiving glucose infusion (B). Basal and insulin stimulated OGT (C) and GFAT1 (D) quantification before (black bars) and after (white bars) 3 days of glucose infusion and representative blots (E). Data represent mean ± standard error and were analyzed using two-way mixed model (group x clamp; group x infusion) ANOVA.

177x185mm (150 x 150 DPI)

SUPPLEMENTAL FIGURES

Supplemental Figure S1.

Plasma glucose (A), plasma radioactivity DPM (B) and plasma glucose specific activity (C) during the 30 minutes prior to the start of the insulin clamp at baseline (circles) and following three days of glucose infusion (triangles). ***P<0.001 vs baseline; n=20 subjects.

Supplemental Figure S2.

Basal (black circles) and insulin-stimulated (open circles) skeletal muscle glucose-6-phosphate, glycogen synthase phosphorylation and GSK3β phosphorylation in FH-, FH+ and CON subjects at Baseline and following three days of glucose or saline infusion.

Figure S1

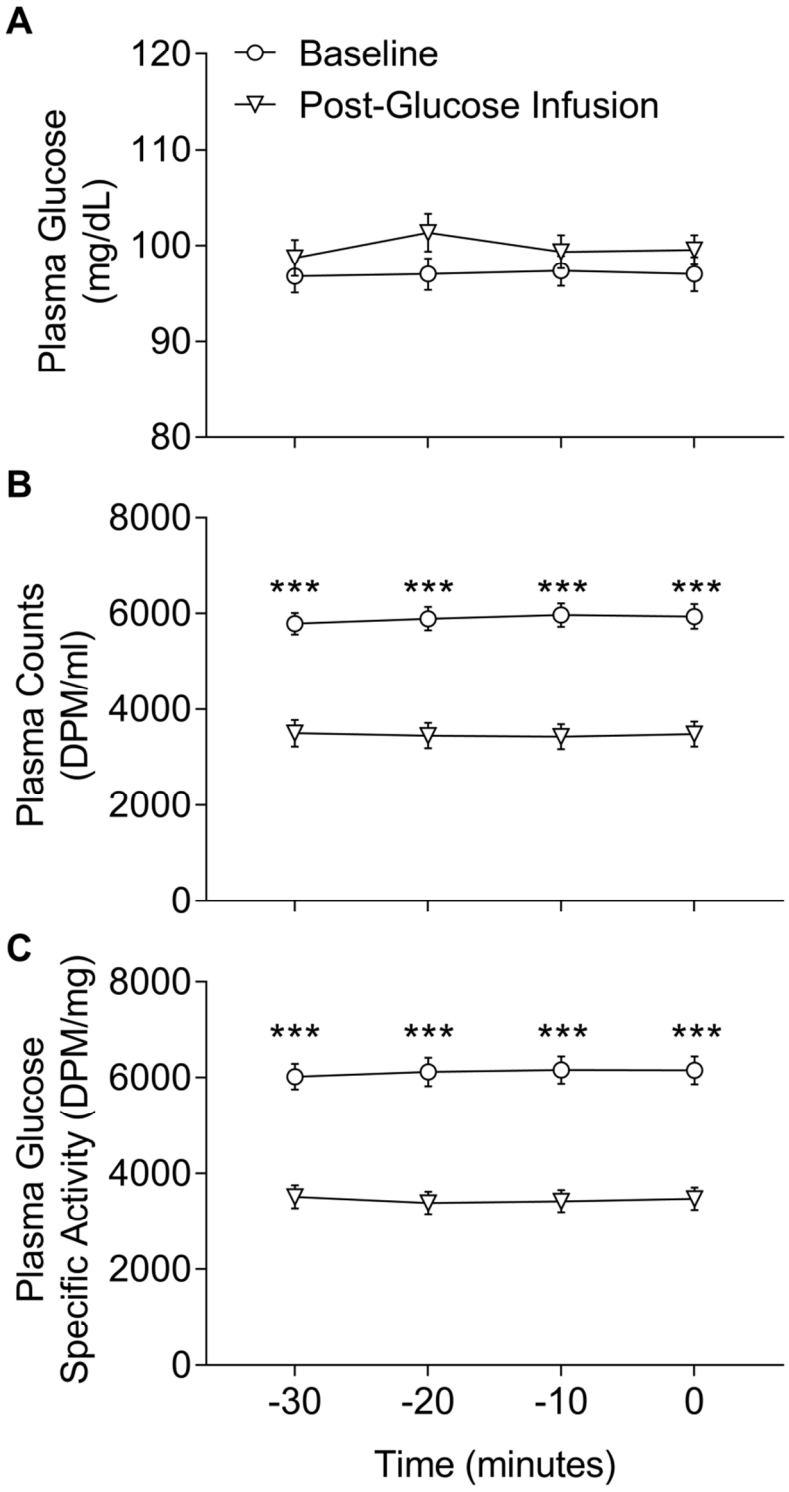
A
Baseline
Post-Glucose Infusion
Plasma Glucose (mg/dL)
120
110
100
90
80
B
Plasma Counts (DPM/ml)
8000
6000
4000
2000
0
***
***
***
***
C
Plasma Glucose Specific Activity (DPM/mg)
8000
6000
4000
2000
0
***
***
***
***
-30
-20
-10
0
Time (minutes)

Figure S2

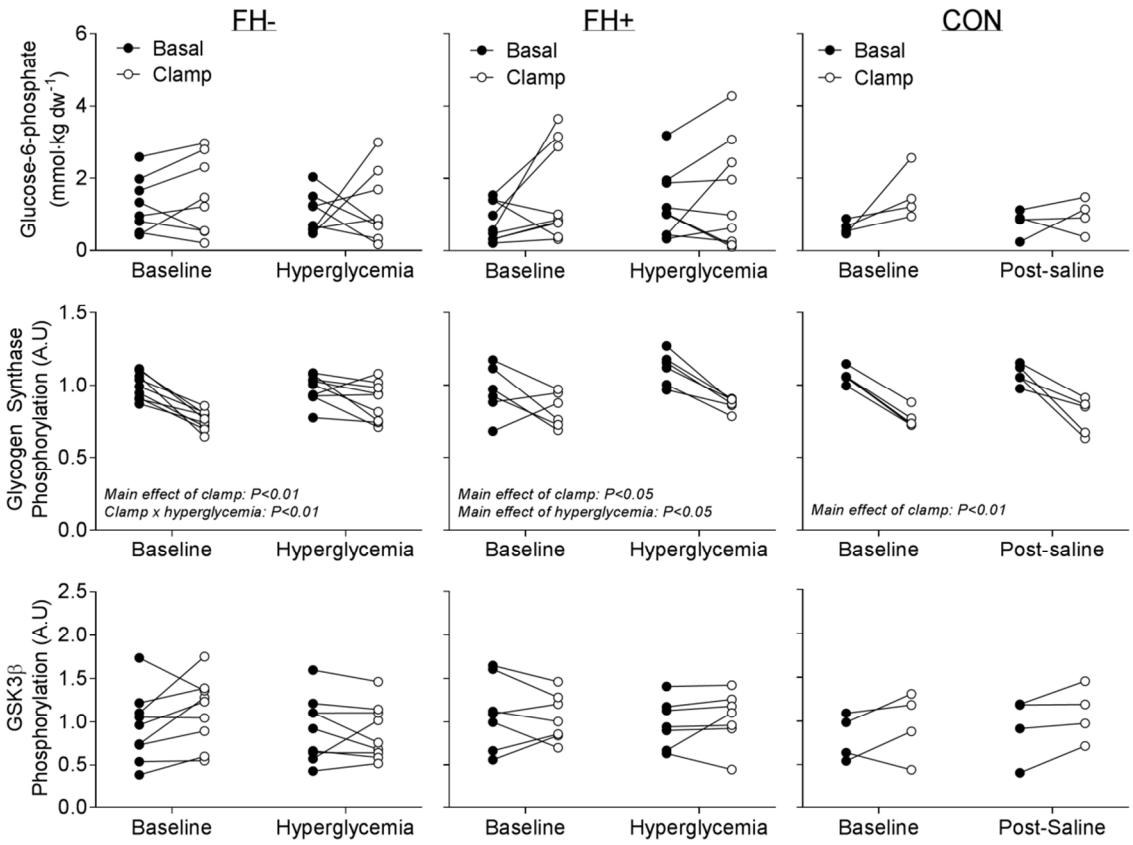
FH-
FH+
CON
Basal
Clamp
Glucose-6-phosphate (mmol·kg dw-1)
Glycogen Synthase Phosphorylation (A.U)
GSK3β Phosphorylation (A.U)
Main effect of clamp: P<0.01
Clamp x hyperglycemia: P<0.01
Main effect of clamp: P<0.05
Main effect of hyperglycemia: P<0.05
Main effect of clamp: P<0.01
Baseline
Hyperglycemia
Post-saline
Post-Saline